Droplet Dynamics on Patterned Surface

Project report submitted to the
Indian Institute of Technology Kharagpur
in partial fulfillment for the award of the degree
of

Master of Technology (Hons.)
in
Chemical Engineering

By

Gaurav Agarwal
15CH30043

Under the guidance of
Prof. Sunando DasGupta

DEPARTMENT OF CHEMICAL ENGINEERING

INDIAN INSTITUTE OF TECHNOLOGY KHARAGPUR

MAY 2020

CERTIFICATE

This is to certify that the project titled "**Droplet Dynamics on Patterned Surface**" is a bonafide record of the work carried out by Gaurav Agarwal (15CH30043), under my supervision and guidance for the partial fulfilment of the requirements for the degree of Master of Technology (Hons.) in Chemical Engineering during the academic session 2019-2020 in the Department of Chemical Engineering, Indian Institute of Technology Kharagpur.

Prof. Sunando DasGupta
Dept. of Chemical Engineering
IIT Kharagpur

DATE:

PLACE: IIT KHARAGPUR

Table of Contents

Abstract

In recent years, there has been a significant investigation in droplet microfluidics, and droplet splitting, in particular, owing to its immense applications in areas of drug discovery, high-throughput screening, nanotechnology, lab-on-chip devices, and material synthesis. The existing techniques are marred, either for their need for an external power source or expensive reagents and elaborate facilities. In the present study, we have used an efficient and novel technique for substrate fabrication which can thereafter be exploited to split droplets using the alternating wettability contrast (up to 100°). In essence, a micro-sized water droplet is dispensed on the hydrophobic region, neighboring hydrophilic regions on both sides, and splitting is observed. The motion of such a droplet has been understood as the superposition of sliding of the center of mass and the spreading of the droplet perimeter initially, leading to its splitting into two daughter droplets and their subsequent motion. The dependence of the droplet splitting process on the wettability difference, $\Delta\theta$, has been investigated. The velocity was analyzed as a function of $\Delta\theta$, while also considering minimization of energy.

Introduction

Motivation

Droplet motion on solid surfaces has been studied for a long time. In recent years, there has been a significant investigation in droplet microfluidics, which is generally described as the creation and manipulation of defined droplets in an insoluble continuous phase. This interest can be attributed to its immense applications in areas of biotechnology, analytical instrumentation, high-throughput screening, and other instrumentation development[1][2]. Droplet manipulation in microfluidic channels using surface acoustic waves has been explored previously[3]. Electrical energy has also been employed extensively as a source of electromechanical actuation of a droplet on a digital microfluidic platform[4][5]. This has been achieved by various means such as those of air pressure, dielectrophoresis[6], electrostatic[7], thermal, and optical control of surface tension forces[8]. However, these methods require external energy to split the droplet and the subsequent motion. It is in this scenario that gradient surfaces emerge as an alternative to obtain sustainable micro-droplet movement by modifying the substrate properties and thereby eliminating the need for an energy source. Different methods employing chemical treatment using fluoroalkyl silane, siloxane, and chlorosilane have been chosen to modify surfaces for creating continuous wettability gradient[9]. However, the whole fabrication procedure needs either various materials or strict reactive conditions, which makes the preparation complicated and expensive.

Objective

In the present study, we aim to use a simple and novel technique for substrate fabrication which can thereafter be used to split the droplet using the alternating wettability gradient effects.

Therefore, development of a process that establishes wettability contrast by control of physical structure is easy-to-implement, is widely applicable to a variety of materials, and can form mechanically stable patterns is of considerable interest.

Further, investigate the behaviour of liquid droplets on such chemically stripped patterned surfaces, considering the minimization of energy.

Theoretical background

Droplet splitting on a substrate with alternating wettability can be better understood by analyzing different forces acting onto the droplet. The net driving force required to split the droplet comes from the balance of capillary force by the viscous drag. The capillary force results from the surface energy gradient typically achieved by controlled chemical modifications of the substrate. Experimental motion studies also reveal that the velocities depend linearly on the radius of the wetted area; moreover, the droplet will move to the hydrophilic region only when the radius is above a certain critical value. The droplet velocity is generally determined by the balance of driving capillary and opposing viscous forces.

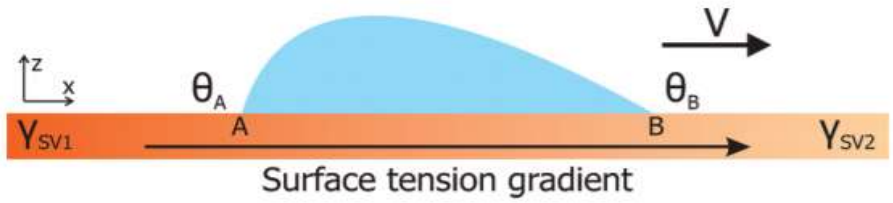

Figure 1. Schematic representation of a sessile droplet on a wettability gradient changing from hydrophobic to hydrophilic.

The unbalanced Young force F originating from different surface tensions on both sides of the droplet can be given as:

$$F = -\frac{\mathrm{d}U}{\mathrm{d}x} = (\gamma_{sv} - \gamma_{sl})_B - (\gamma_{sv} - \gamma_{sl})_A$$

The difference in surface energies consequently results in different contact angles at points A and B.

The above expression can further be written in terms of local dynamic contact angle as

$$F = \gamma_{lv}(\cos\theta_B - \cos\theta_A)$$

The motion of the droplet is hindered by viscous drag i.e. friction force Fη. Using the lubrication approximation and assuming a circular shape of the wetted area (with radius R), it is given by:

$$F_\eta = 3\eta\pi RV \int_{x_{min}}^{x_{max}} \frac{\mathrm{d}x}{\xi(x)}$$

Simulation

Model Setup

Surface Evolver is a finite element-based software for studying surfaces confined by the energies such as surface tension, gravitational energy, and user-define surface integrals. In SE, a surface is implemented as a union of triangles formed by connecting vertices. Increasing the number of those geometric elements results in more accurate results of the simulation.Fig.2 shows the surfaces formed by the vertices, edges, faces and body. Generally, the number of vertices can be increased for better accuracy of the shape. The surface prescribed to a set of constraints in SE will be evolved towards its minimal energy using a gradient descent method. A detailed description of the technical procedure can be found in the SE manual[10].

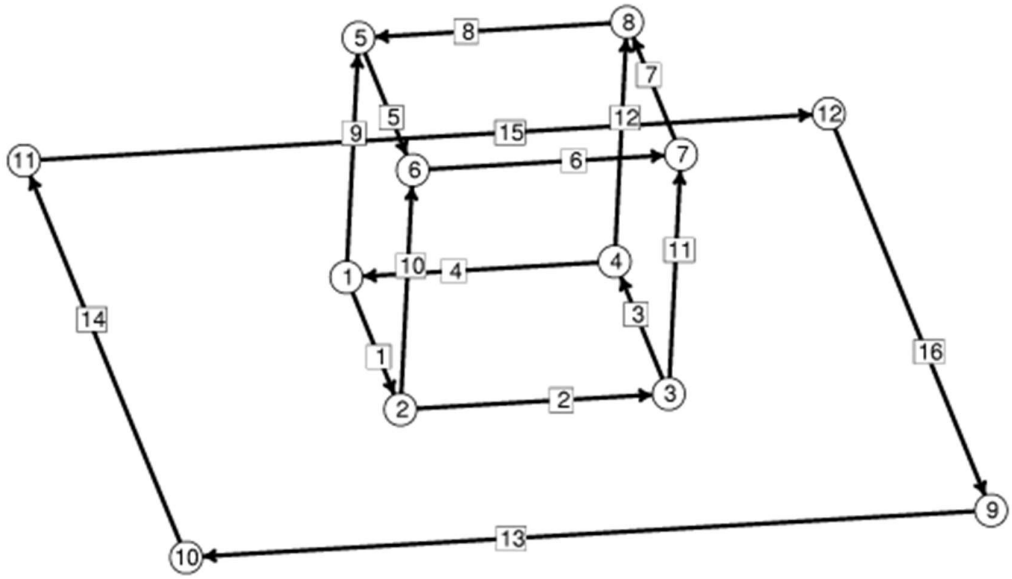

Figure 2. Representation of the surface by its vertices, edges, faces and body.

In this work, the wetting behaviour of a droplet on chemically striped surfaces is simulated. The initial shape of the droplet in our simulation is defined as a cube, as shown in Fig. 3. Fig. 3 shows the initial state of the droplet with the volume of 5μL residing on top of hydrophobic stripe. As defined in the figure, the stripes in yellow have the intrinsic CA of θ1 and the width of sw, and the grey stripes represent those with intrinsic CA of θ2. In this study, θ1 is always

higher than θ2, and from now on, yellow and grey stripes are referred to as hydrophobic and hydrophilic stripes, respectively. The table shows the corresponding values of the dimensions used in figure 2.

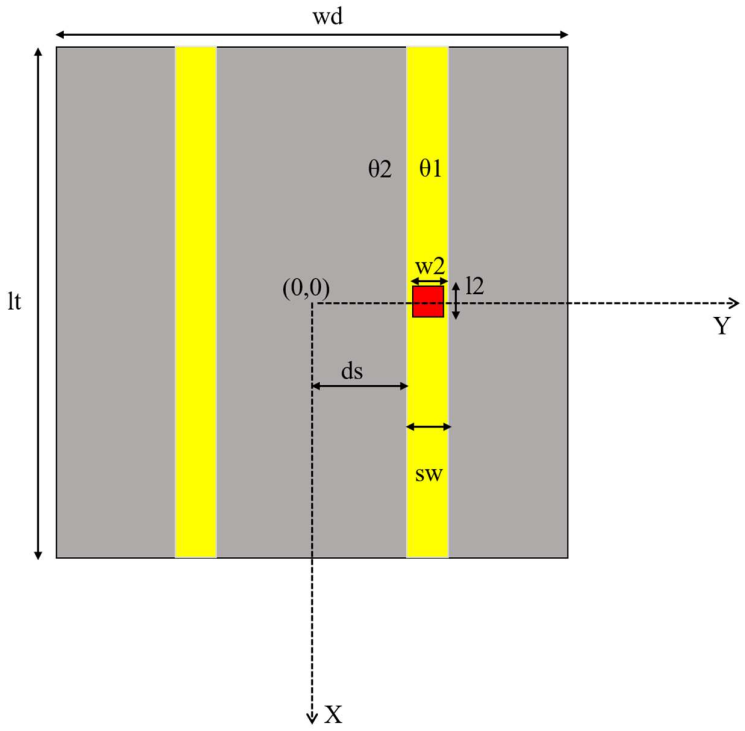

lt	0.025
wd	0.025
ds	0.0035
sw	0.002
l2	0.00136
w2	0.00136
h2	0.00136
d2	0.0001
VOL	5* 10^-9
θ1	110°
θ2	30°

Figure 3. Initialised surface along with the corresponding dimensions (in SI units).

For the system of a droplet on chemically striped patterned surfaces, the total FE of the system calculated in SE is calculated by the equation

$$\frac{F}{\gamma_{la}} = S_{la} - \iint_{S_{sl}} cos\theta_1 dxdy - \iint_{S_{sl}} cos\theta_2 dxdy$$

Where S_{la} and S_{sl} represent the liquid–air and solid–liquid interface area, respectively; γ_{la} stands for the liquid–air interfacial tension. Here, FE is normalized by γla, referred to as relative free energy hereafter. The intrinsic CA θ_1 and θ_2 hydrophobic and hydrophilic strips are defined by Young's equation:

$$\gamma la\, cos\theta i = \gamma sa - \gamma sl$$

where γ_{sa} and γ_{sl} are the solid–air and solid–liquid interfacial tensions.

Gravity is ignored since droplet volume is kept sufficiently small for simulation to minimize the effect of gravity. Three-phase contact line tension is also neglected since the accumulated contact line energy is small enough compared to the total energy of the system. In our case, the facets that come in contact with striped surfaces are deleted since those facets are not needed and may get in the way, as recommended by Brakke[10]. The so-called "multiple one-sided constraint" is used to compensate the FE of the deleted facets using user-defined line integrals. In addition, other two kinds of constraints are used in simulation: the geometric constraint that ensures the constant droplet volume during the evolution process; and the constraint that confines vertices to stay in the corresponding boundaries between stripes. The values of 1, $-\cos\theta 1$, and $-\cos\theta 2$ are assigned to the liquid–air, hydrophobic stripe–liquid, and hydrophilic stripe–liquid interfaces according to eqn (1). The surface tension assignment is also shown in Fig. 1b. Assume that the normal of deleted the facet as S, we need a vector field w that satisfies the following equation for line integral:

$$\int_{face\ 6} T\ k \cdot dS = \int_{\text{bdry of face 6}} w \cdot dl$$

where T is the surface tension of the deleted facets; and it is $-\cos\theta 1$ for wet stripes and $-\cos\theta 2$ for dry stripes. Thus, either [w with combining right harpoon above (vector)] = −Tyi or [w with combining right harpoon above (vector)] = −Tyj can be selected for the line integrals along the three-phase contact line, where i, j, k are the unit basis vectors.

Result and Discussion

In an effort to study the effect of the volume of the droplet on splitting, the simulation is performed for volumes from 1 to 10μL. It is observed that as long as the volume of the dispensed drop is such that the diameter of the footprint of the droplet is less than than the width of the hydrophobic strip, the droplet stays within the region. The critical value of the volume of droplet required for splitting was obtained to be 4μL. Therefore, a volume of 5 μL is chosen for splitting experiments.

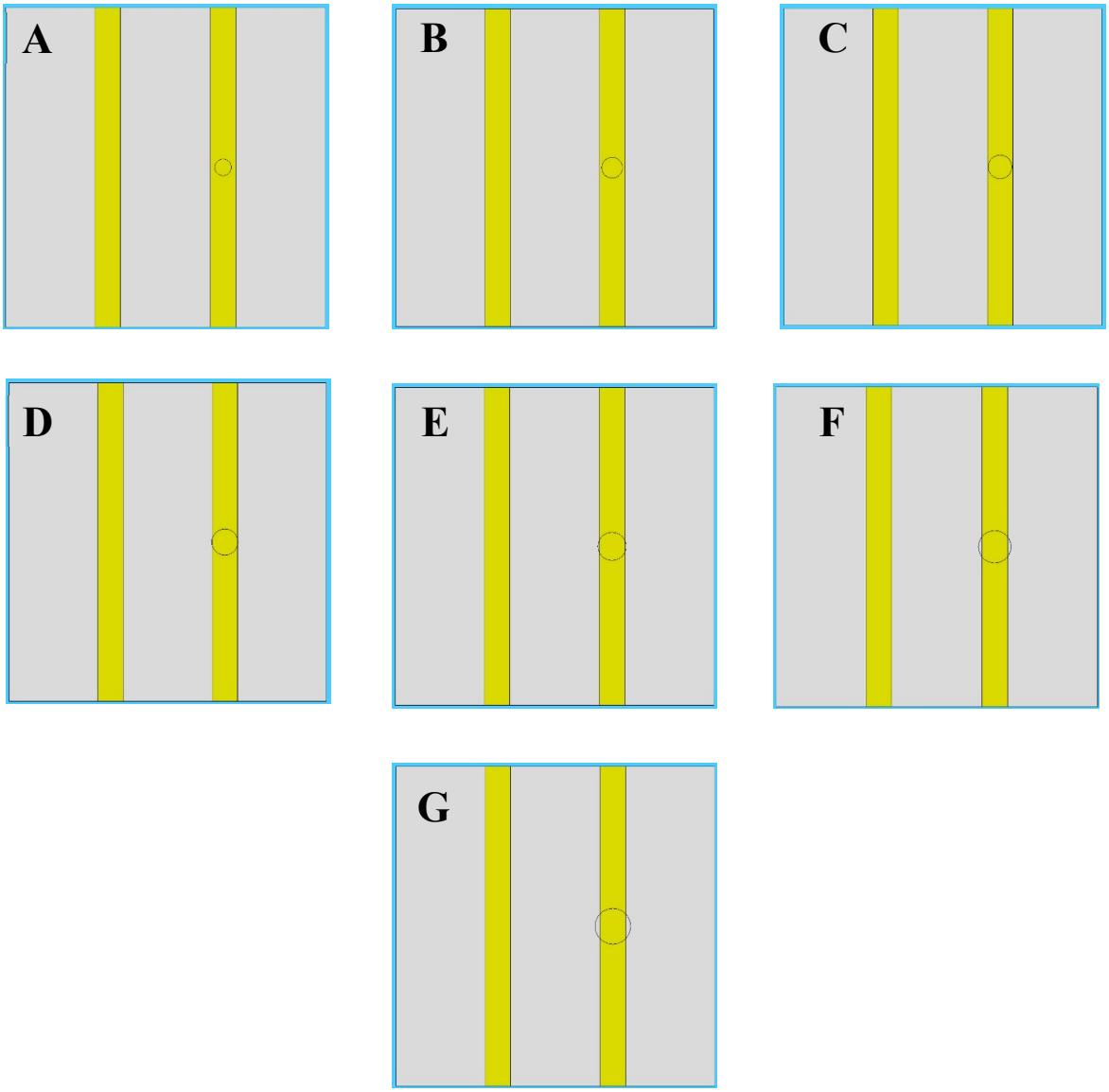

Figure 4. Bottom view of the substrate for droplet volume of (a) 1 μL (b) 2 μL (c) 3 μL (d) 4 μL (e) 5 μL (f) 7.5 μL (g) 10 μL.

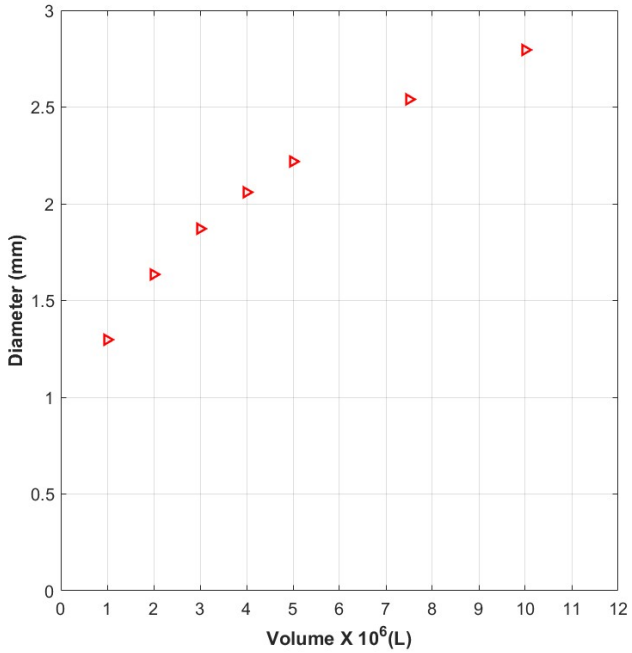

Figure 5. The values of the diameter of the footprint corresponding to different volume of droplet.

It was noted that when a 5 µL droplet was dispensed on the substrate with the CAs 30º and 110º at the hydrophilic and hydrophobic regions respectively, it can be observed that the contact angle in the perpendicular directions, and an elongated shape is obtained.

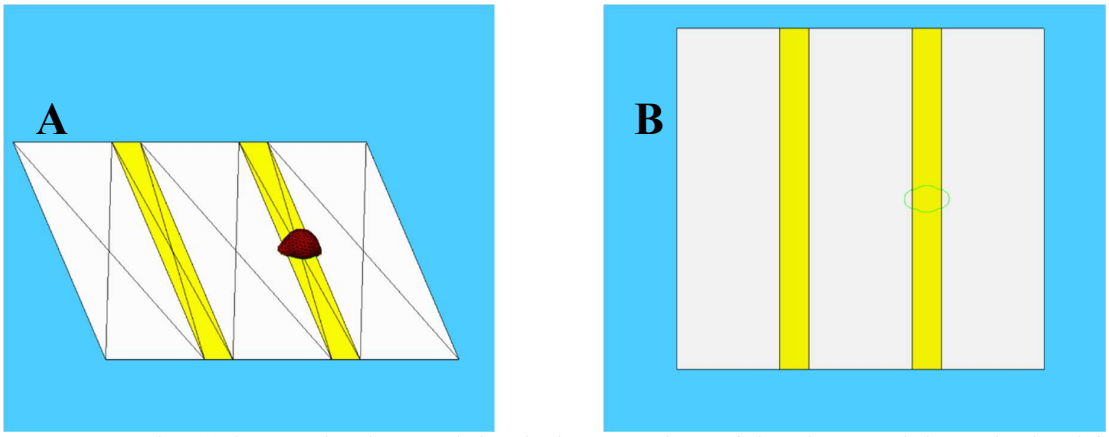

Figure 6. The (a) isometric view and the (b) bottom view of the elongated drop obtained for values of CAs 30º and 110º at the hydrophilic and hydrophobic regions respectively.

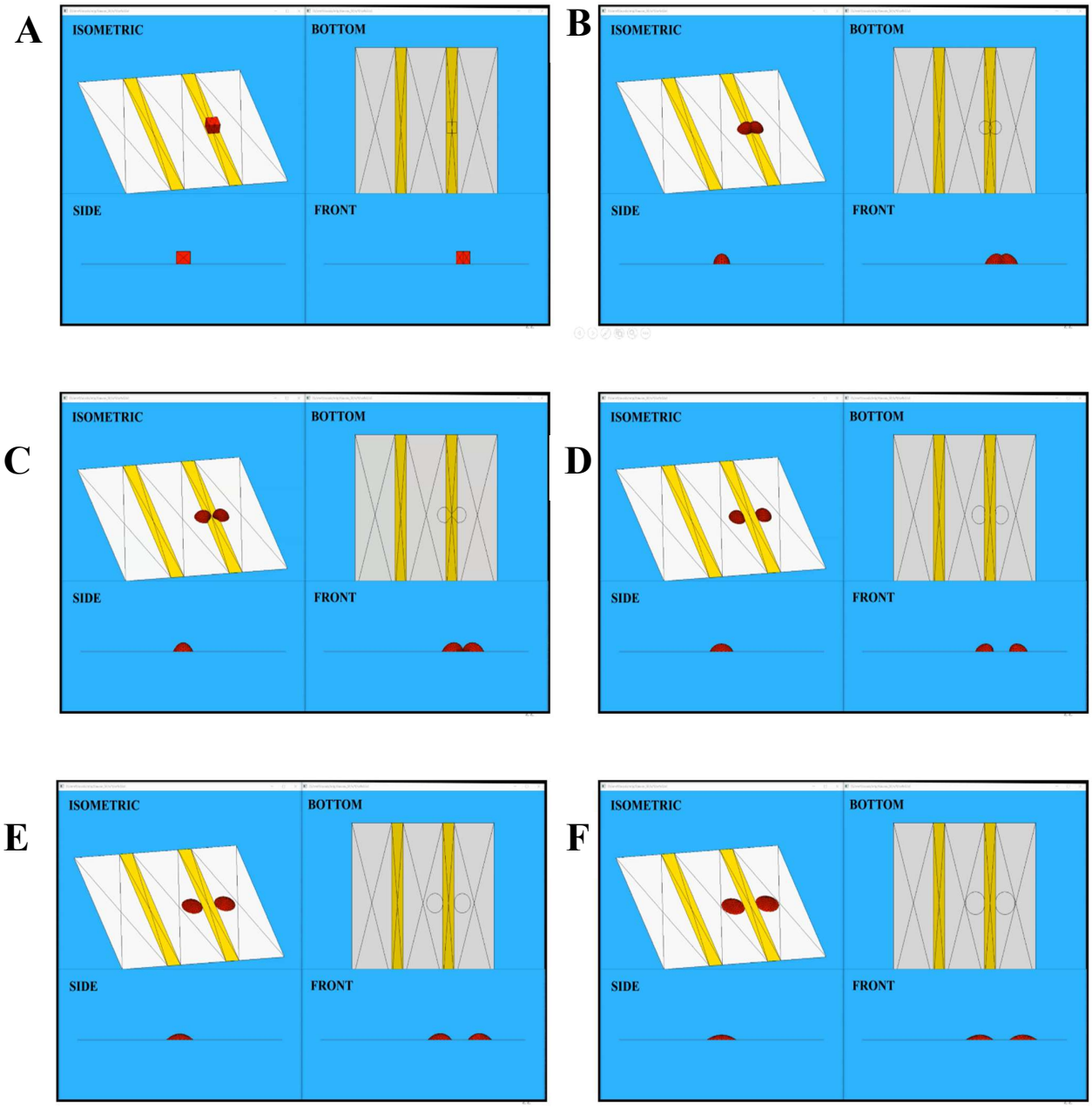

Figure 7. The progression of droplet splitting obtained for values of CAs 30º and 110º at the hydrophilic and hydrophobic regions respectively.

Fig.7 shows the progression of droplet motion from A to F. After the splitting is complete the geometry is obtained a shown in figure 8. Both the daughter droplets have moved to the hydrophilic region.

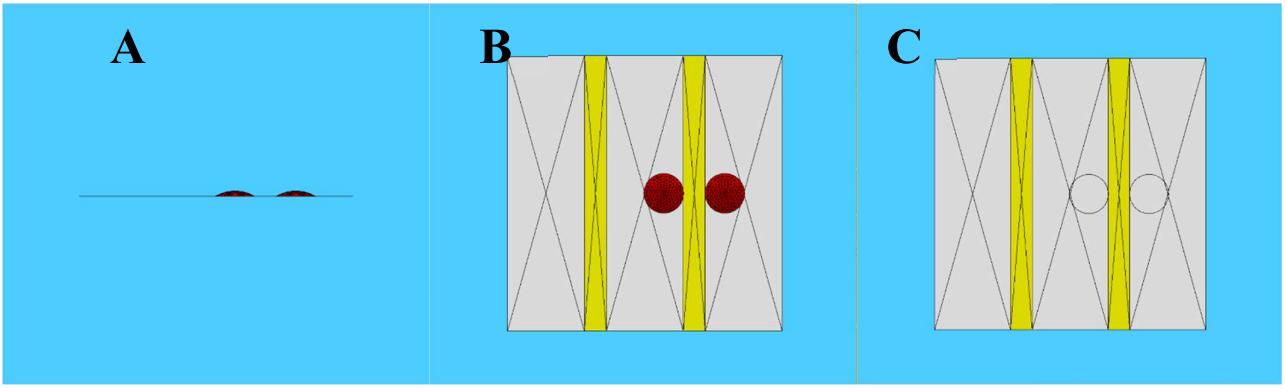

Figure 8. The (a) front view (b) top view and (c) bottom view of the two daughter droplets obtained after splitting.

We have developed the model to predict the contact angles and elongation of a droplet on a chemically defined anisotropic patterned surface, for different liquids and substrate wettability.

Experimental Methods

Substrate fabrication and characterization

Glass slides are used as a substrate for the experiments. Stripes of 25mm × 25mm with no visible scratches are cut from glass slides and are cleaned ultrasonically with acetone and de-ionized water for 10 minutes each. The cleaned glass slides are then dried in a hot oven at ~95 ^{0}C to make them moisture free. These moisture free slides are then spin-coated with Sylgard 184 which is chemically polydimethylsiloxane (PDMS). To prepare substrates with different elasticity, the base to the cross-linker ratio of Sylgard 184 is varied as 10:1, 30:1 and 50:1. This coating also renders the fabricated substrates hydrophobic.

Preparation of wettability contrast patterns

The hydrophobic glass slides are covered with equally spaced stripes of parafilm (Pachiney Plastic Packaging, USA) (width~2 mm) in the vertical directions, as shown in Figure 2.

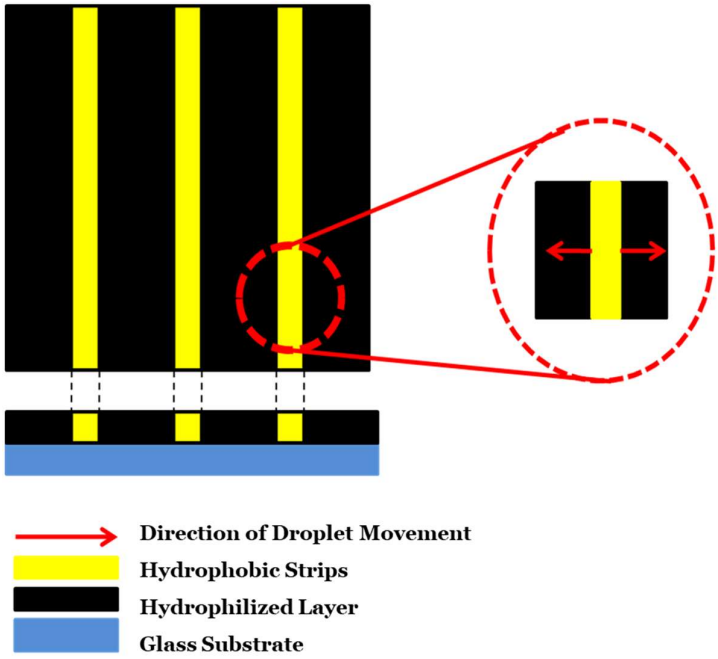

Figure 9. Schematic of the wettability contrast pattern and direction of the ensuing droplet motion.

The substrate with parafilm stripes is then exposed for 60 seconds using a Harrick Plasma cleaner (Harrick Plasma, PLASMAFLO PDC-FMG). The plasma treatment makes the uncovered surfaces relatively hydrophilic with a water contact angle of around 5º. The portions covered with parafilm stripes retain their hydrophobicity with a water contact angle of around 110º – 115º. Goniometer (dataphysics, OCA 15 Pro) is employed for contact angle measurements in all cases.

Droplet splitting

The parafilm stripes are then carefully removed, thus we are now left with a substrate with vertical hydrophobic stripes having hydrophilic surroundings on both sides. DI water (5µl ± 0.2µl) is dispensed at the center of the strip using a motorized dispensing unit. The droplets after being deposited onto the substrate, encounter the wettability contrast zone which provides a necessary driving force to initiate droplet movement. The droplet prefers to move to hydrophilic zones present on both sides causing parent droplet to split into two smaller symmetrical droplets. The droplet dispensing and motion is recorded using a high-speed camera (Phantom, v411) at 5000fps (1280×720 pixels). Experiments are repeated several times

with all type of substrates to confirm its reproducibility. The recorded videos are further analyzed to get droplet velocity.

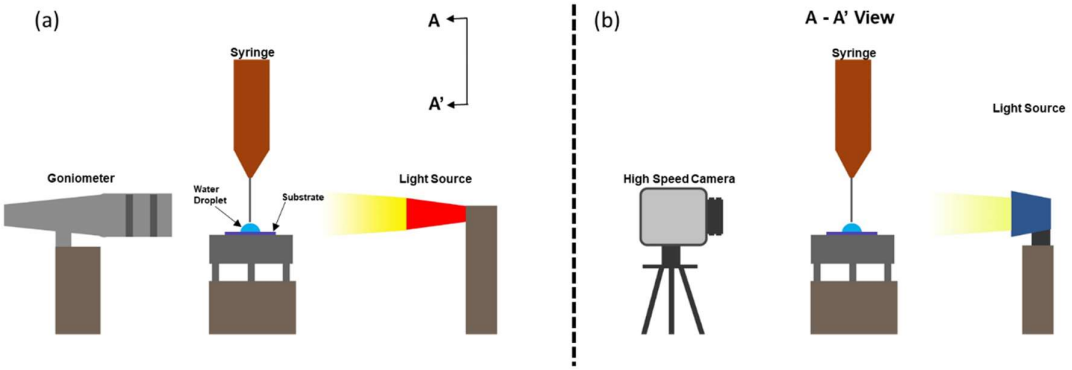

Figure 10. Schematic of the (a) front and (b) side view of the experimental configuration for the droplet splitting.

The edge in contact with the hydrophilic region is termed as the leading edge while the other edge is termed as the receding edge. The droplet's first point of contact is considered as the origin of the system and the direction in which the leading edge moves is taken to be the positive x-axis.

Results and Discussion

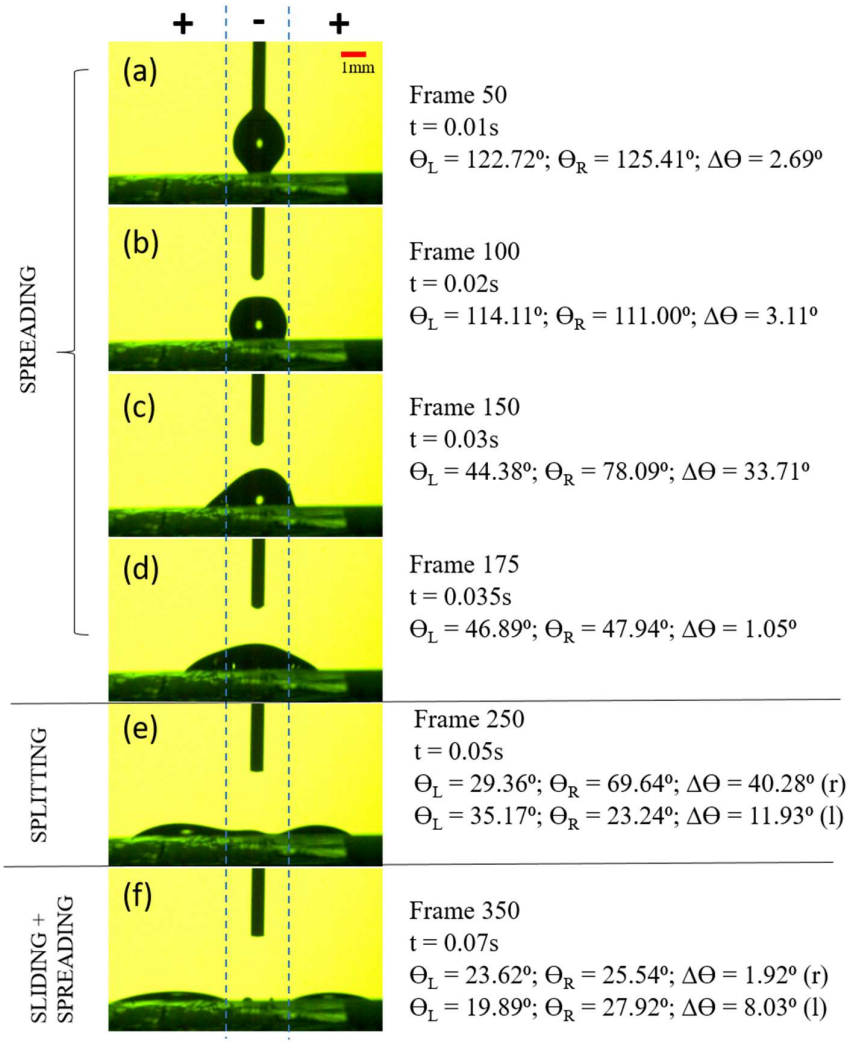

Figure 11. Images are taken from a high-speed camera showing the side view of droplet motion (wettability difference = 100º). The values for dynamic CAs on the right (θ_R) edge and left (θ_L) edge during different regimes are presented. Vertical dashed lines indicate the borders between different wettability regions, as introduced in Figure 2. + indicates the hydrophilic regions whereas – indicates the hydrophobic region.

Figure 11(a) shows that the droplet has a symmetrical shape. In figure 11(b) the syringe - droplet neck breaks and the droplet maintains its symmetrical shape. The droplet assumes an asymmetrical shape because of spreading of the left side over the hydrophilic region as shown in figure 11(c). The droplet regains its symmetrical shape due to the flow of liquid from the side of larger curvature towards smaller curvature. It spreads over to both hydrophilic regions.

This is shown in figure 11(d). In figure 11(e) the droplet starts to split and a neck forms. The breaking of this liquid bridge marks the end of the first regime. Subsequently, there are two similar daughter droplets which are present in only the hydrophilic regions as shown in figure 11(f).

In an effort to study the effect of wettability difference on droplet velocity, the experiment is performed for two wettability differences of 100º and 60º. PDMS coated glass slides are exposed to varying durations of plasma treatment. By treating the substrate at high plasma setting for 1 minute a wettability of 9-10º, whereas upon treatment at low setting for 30 seconds a wettability of 49-50º degree was achieved. The paraffin covered strip which was unexposed to plasma maintained a contact angle of 110º. The variation in velocity is examined as a function of wettability difference only. Table 1 shows the different conditions for obtaining various wettability difference.

Hydrophobic		**Hydrophilic**		**CA Difference**	**Remark**
Plasma	**CA**	**Plasma**	**CA**		
I	110	High(O_2 – 30s) 1 min	9-10	100	Very fast splitting
II	110	Low 150mtorr (No O_2) 30s	49-50	60	Slower than I
III	110	Med 150mtorr 30s	25-27	83	Splitting
IV	110	Low 150 20s	48-49	61	Unseen splitting
V	110	'' gap + 10s	44-45	65	
VI	110	Low 150 20s (No O_2)	38-40	70	1mm strip

Table 1. Plasma treatment conditions for obtaining various wettability difference for droplet splitting.

Regime 1: Before the liquid bridge breaks

In the first regime, there is no translation of the COM of the droplet. Hence, the average velocity is calculated as the rate of change of radius with time.

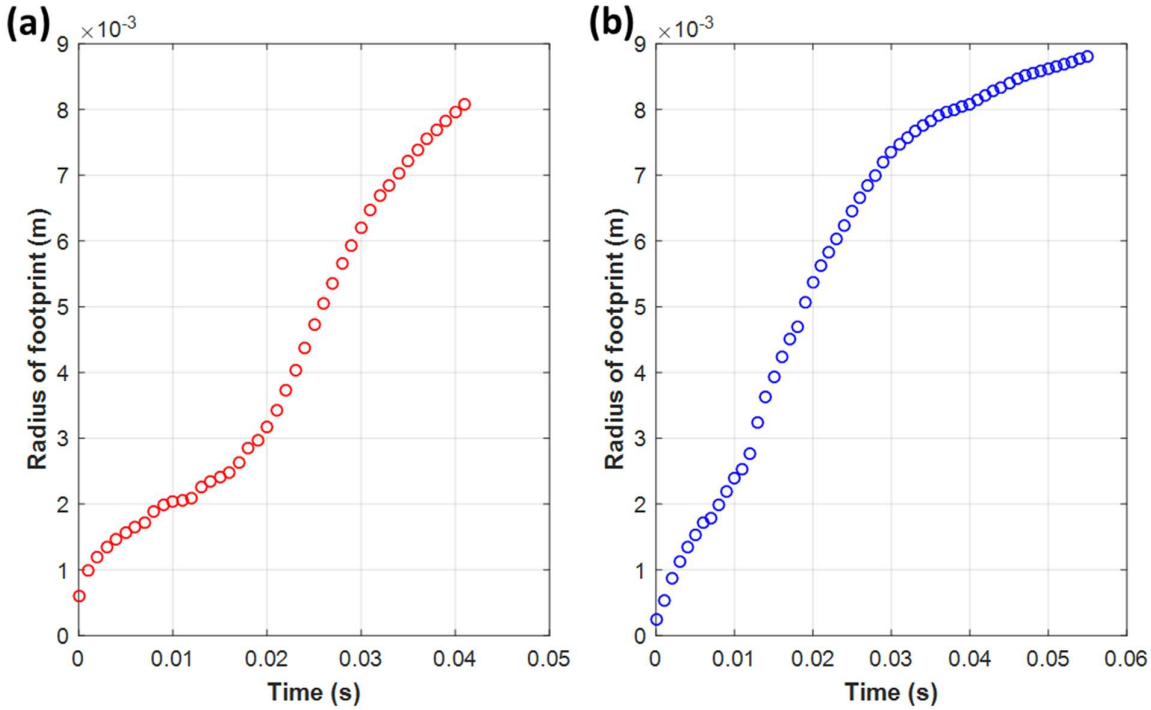

Figure 12. (a) For a wettability difference of 100º, the radius of footprint with time. (b) For a wettability difference of 60º, the radius of footprint with time.

Wettability Difference	Increase in radius	Time Taken	Average Velocity
Δθ	ΔR (m)	Δt (s)	$\frac{\Delta R}{\Delta t}$ (m/s)
100º	7.49E-03	4.10E-02	1.83E-01
60º	8.56E-03	5.50E-02	1.56E-01

Table 2. Summary of the effect of wettability on average velocity.

Result

A higher value of average velocity is observed for higher wettability difference. From 0.156 m/s at 60º difference to 0.183 m/s at 100º difference.

Regime 2: After the liquid bridge breaks

The motion of the daughter droplet can be visualized as the superposition of two processes. The sliding of the COM of the droplet along with the spreading of the droplet perimeter, with each point on the perimeter moving with the same velocity at an instant.

Velocity of Edge = Sliding Velocity of COM + Spreading Velocity of the Perimeter

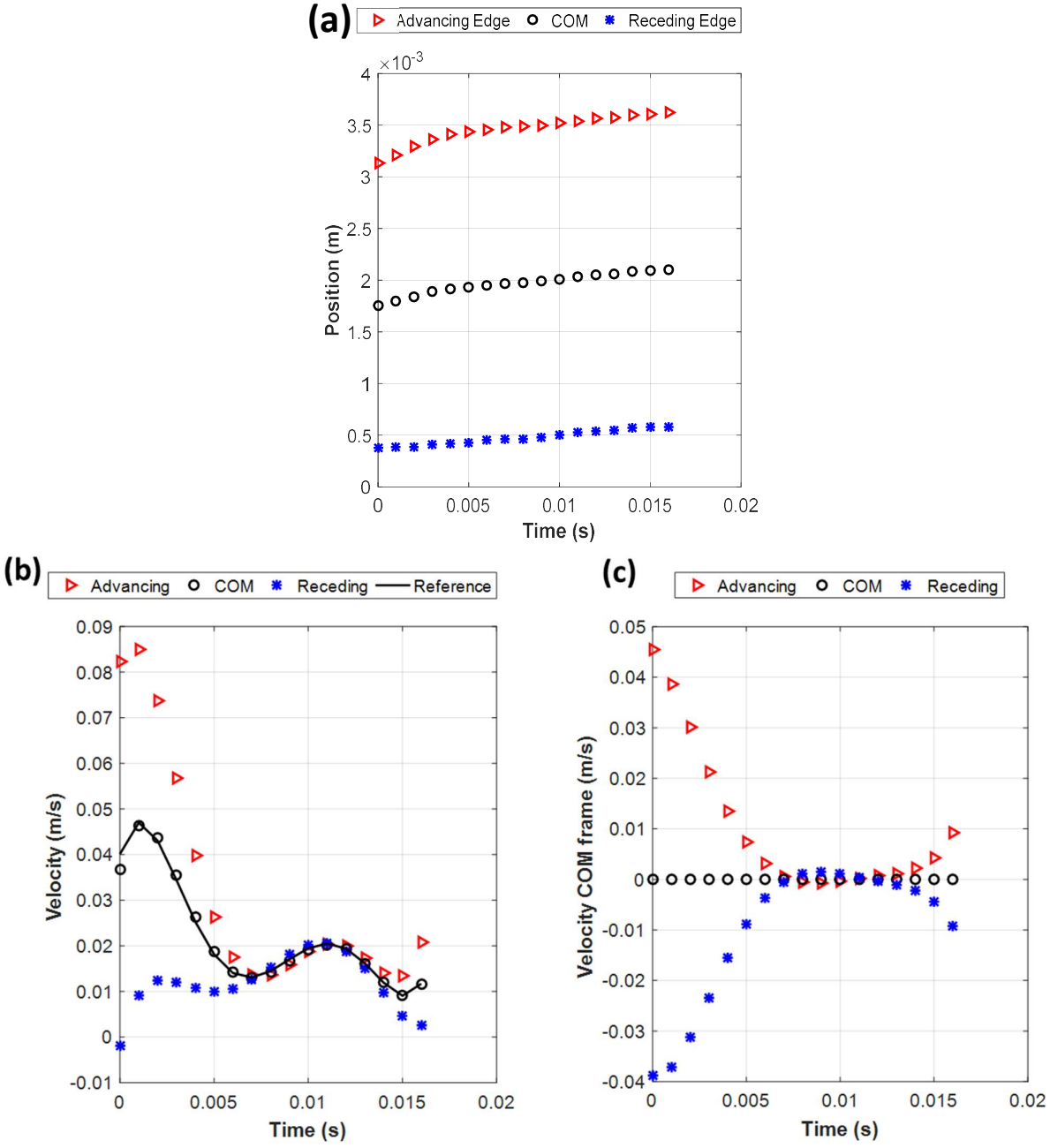

Figure 13. (a) For a wettability difference of 100º, the evolution of the left (receding, blue stars) and right (advancing, red triangles) edges as a function of time; the center position (black circle) is the average of both edges. The middle of the syringe is taken as the zero position on

the surface. (b) Time evolution of the x-component of velocity for the same system. Reference line shows the average of the advancing and receding edge velocities. (c) Time evolution of the x-component of velocity for the same system in COM frame.

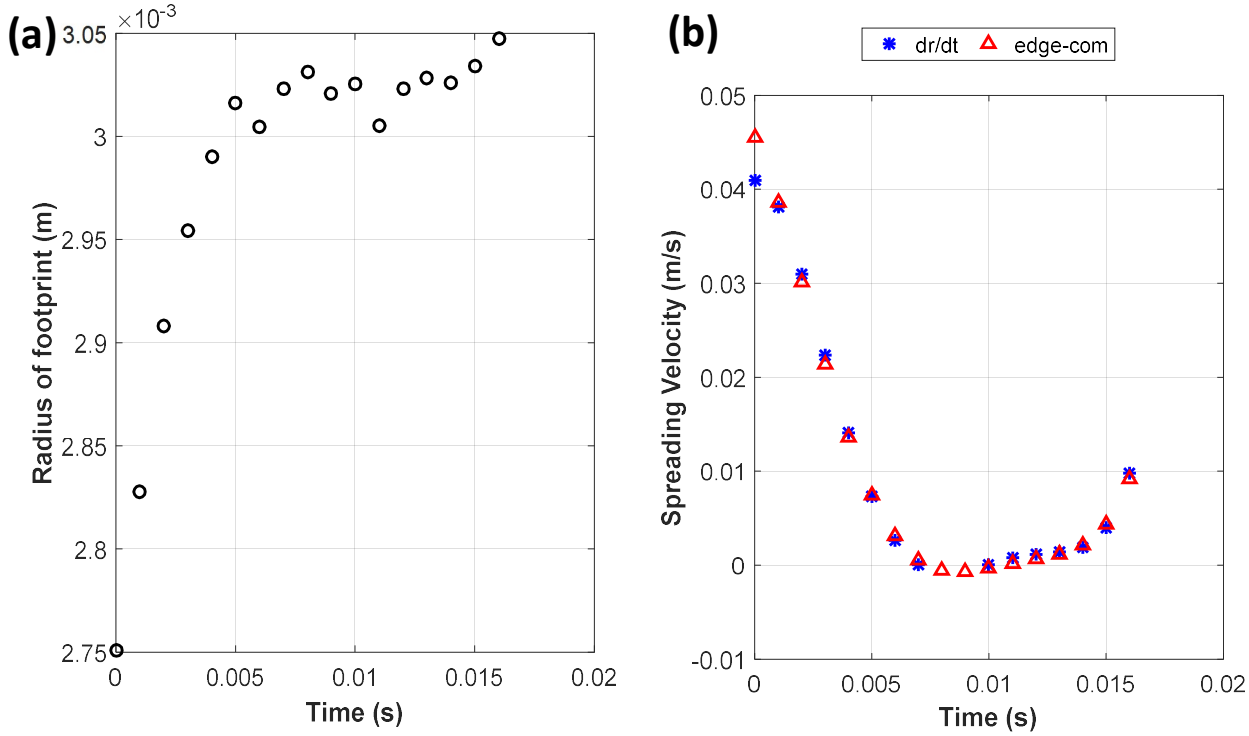

Figure 14. For a wettability difference of 100º, the time evolution of the radius of the footprint. (b) Spreading velocity comparison.

	Initial	**Final**
Radius of footprint	2.699E-3 m	3.593E-4 m
Height	3.045E-3 m	2.819E-4 m

Table 3. Summary of the radius of footprint and height.

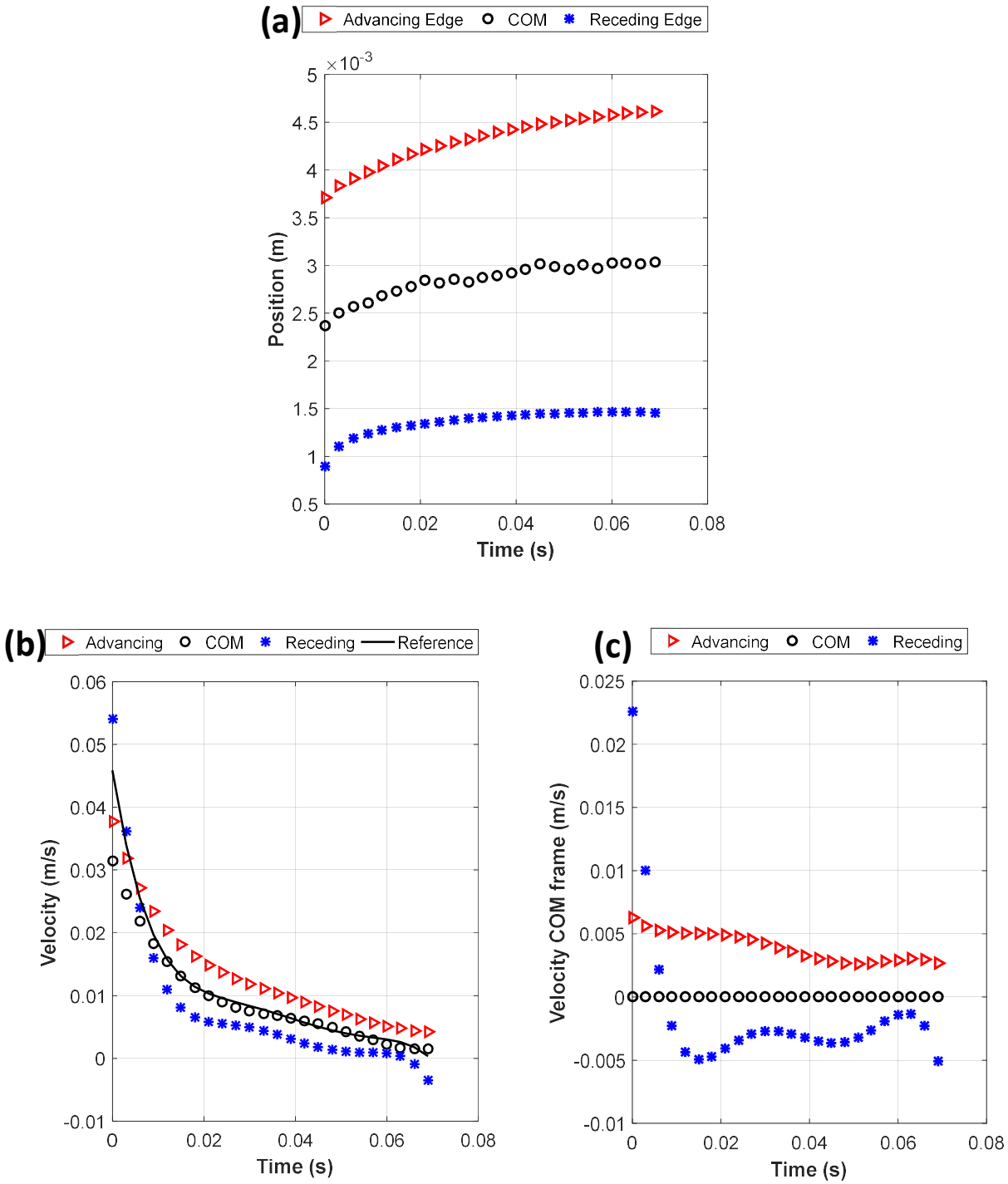

Figure 15. (a) For a wettability difference of 60º, the evolution of the left (receding, blue star) and right (advancing, red triangle) edges as a function of time; the center position (black circle) is the average of both edges in COM frame. (b) Time evolution of the x-component of velocity for the same system in COM frame. (c) Time evolution of the x-component of velocity for the same system in COM frame.

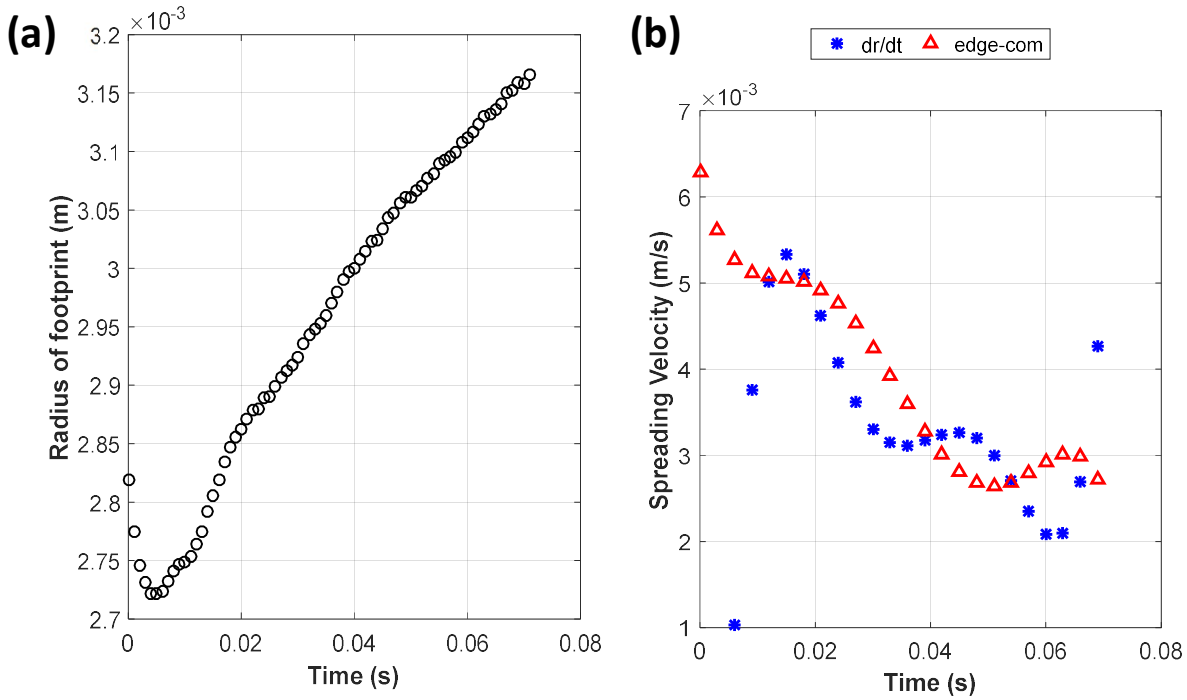

Figure 16. For a wettability difference of 60º, the time evolution of the radius of the footprint. (b) Spreading velocity comparison.

	Initial	Final
Radius of footprint	2.974E-3 m	3.321E-3 m
Height	5.749E-4 m	3.344E-4 m

Table 4. Summary of the radius of footprint and height.

Analysis

From figures 13(a) and 15(a), the positive slope of the position vs time graph confirms the sliding of the COM. Figures 13(b), 15(b) and 13(c),15(c) the sliding velocity of the COM and the spreading velocity of the perimeter can be observed, respectively. Tables 3 and 4 show the increase in the droplet radius and decrease in droplet height implying the spreading.

Conclusion

Using surface evolver simulations as mentioned in this work, has enabled us to predict the contact angles, splitting and subsequent motion of a droplet on a chemically patterned surface with alternating wettability. The model though developed for water can be easily adapted for other liquids as well. This allows us to effectively design and optimize chemically striped patterned surfaces for the experiments.

In the experiments we have demonstrated that when a micro-sized water droplet is dispensed on the hydrophobic region with neighboring hydrophilic regions on both sides, splitting can be observed. The motion of such a droplet has been understood as the superposition of sliding of the center of mass and the spreading of the droplet perimeter initially, leading to its splitting into two daughter droplets and their subsequent motion. The dependence of the droplet splitting process and velocity on the wettability difference, $\Delta\theta$, has been investigated.

References

[1] R. D. Smith and R. T. Kelly, "Controlled dispensing and mixing of pico- to nanoliter volumes using on- demand droplet-based microfluidics Controlled dispensing and mixing of pico- to nanoliter volumes using on-demand droplet-based microfluidics," no. November 2015, 2013.

[2] C. Yang, W. Wang, A. M. Grumezescu, K. Huang, and Y. Lin, "One-step synthesis of platinum nanoparticles loaded in alginate bubbles One-step synthesis of platinum nanoparticles loaded in alginate bubbles," 2014.

[3] J. H. Jung, G. Destgeer, B. Ha, J. Park, H. J. Sung, and J. H. Jung, "On-demand droplet splitting using surface acoustic waves," *Lab Chip*, vol. 16, no. 17, pp. 3235–3243, 2016.

[4] M. G. Pollack, A. D. Shenderov, and R. B. Fair, "Electrowetting-based actuation of droplets for integrated microfluidicsElectronic supplementary information (ESI) available: six videos showing droplet flow, droplet dispensing and electrowetting. See http://www.rsc.org/suppdata/lc/b1/b110474h/," *Lab Chip*, vol. 2, no. 2, p. 96, 2002.

[5] X. Yang, X. Liu, D. W. Hess, and V. Breedveld, “Underwater Oil Droplet Splitting on a Patterned Template,” *Langmuir*, vol. 33, no. 47, pp. 13522–13529, 2017.

[6] B. Wee, B. Wee, M. Kumemura, M. Kumemura, D. Collard, D. Collard, H. Fujita, and H. Fujita, “Isolation of single dna molecule in a picolitre-sized droplet formed by liquid dielectrophoresis,” *Analysis*, pp. 36–38, 2008.

[7] T. Taniguchi, T. Torii, and T. Higuchi, “Chemical reactions in microdroplets by electrostatic manipulation of droplets in liquid media †,” pp. 19–23, 2002.

[8] K. Ichimura, S. Oh, and M. Nakagawa, “Light-Driven Motion of Liquids on a Photoresponsive Surface,” no. June, 2014.

[9] W. T. Choi, X. Yang, V. Breedveld, and D. W. Hess, “Creation of wettability contrast patterns on metallic surfaces via pen drawn masks,” *Appl. Surf. Sci.*, vol. 426, pp. 1241–1248, 2017.

[10] K. A. Brakke, “The Surface Evolver,” 1982.

[11] E. S. Kooij, H. J. W. Zandvliet, B. Poelsema, H. P. Jansen, and O. Bliznyuk, “Smart Design of Stripe-Patterned Gradient Surfaces to Control Droplet Motion,” *Langmuir*, vol. 27, no. 17, pp. 11238–11245, 2011.